

THE FORMATION OF EMISSION LINES IN THE EXPANDING CHROMOSPHERES OF LUMINOUS COOL STARS. I. THE IMPORTANCE OF ATMOSPHERIC EXTENSION AND PARTIAL REDISTRIBUTION EFFECTS

S. A. DRAKE AND J. L. LINSKY¹

Joint Institute for Laboratory Astrophysics, University of Colorado and National Bureau of Standards

Received 1983 January 5; accepted 1983 March 21

ABSTRACT

Most late-type luminous stars are losing mass in cool stellar winds, although the mass-loss rates and mechanisms of these outflows remain uncertain. In many red giants the only evidence for mass loss is the presence of a characteristic asymmetry in the strongest ultraviolet resonance lines, such as the Mg II *k* line. In this paper, we discuss the available methods for treating radiative transfer in such chromospheric lines in an expanding, extended medium and select the comoving frame method (including partial redistribution) as the most suitable. We briefly outline this technique in the context of a two-level atom. Prior to applying this technique to deriving atmospheric properties from observed line profiles, we present some schematic examples to illustrate the sensitivity of the calculated line profiles to the outflow velocity, chromospheric temperature gradient, physical extent of the atmosphere, line-to-continuum strength, and the incoherence fraction. In this paper, we illustrate the difference in the computed line profiles between assuming partial and complete redistribution for a wide range of atmospheric and wind parameters.

Subject headings: line profiles — radiative transfer — stars: chromospheres — stars: late-type

I. INTRODUCTION

Two unambiguous spectroscopic signatures of mass loss from a star are either the presence of a “true” P Cygni profile, defined as a line with an emission component close to the radial velocity of the stellar photosphere and a blueshifted absorption component, or the presence of a simple absorption feature at negative radial velocity. Examples of the former are the Beals’s (1951) Types I, II, IIIb, and IV profiles, and of the latter are the Beals’s Type VIII profile and cases in which there are one or more blueshifted (circumstellar) absorption components in addition to a “stationary” (at the stellar frame of reference) photospheric absorption feature. The presence of these characteristics in a spectrum *definitely* implies mass loss when the radial velocity of the blueshifted absorption exceeds the escape velocity from the stellar surface. When the radial velocity is smaller, then mass loss is very likely present, but it is not possible to rule out an extended outer atmosphere with a circulation pattern of rising and falling elements. The simultaneous presence of redshifted absorption components makes the latter scenario more plausible. With the exception of some T Tauri stars (see, e.g., Rydgren 1977), however, the integrated fluxes of stars rarely show such complex behavior.

Because of their large oscillator strengths and populations, the resonance lines of the dominant ions of common elements such as Ca⁺, Mg⁺, and O are generally most sensitive to mass loss. However, in late-type stars these lines are in emission because they are effectively

thick (Avrett and Hummer 1965) in the chromosphere where the temperature is rising with height. Thus, emission in the line due to a larger geometrical extent of the line formation region compared to that of the continuum, if present, is difficult to distinguish from emission in an effectively thick but geometrically thin chromosphere. Because resonance lines in these stars generally have line source functions that peak in the chromospheric rise region and then decrease farther out, their chromospheric emission profiles typically have a self-reversal, which, if sufficiently broad, may obliterate any P Cygni absorption component. Also, as Ulrich (1976) has pointed out in connection with pre-main-sequence stellar line profiles, a small, blueshifted dip in an emission feature that does not descend to the continuum level (e.g., a Beals’s Type IIIa profile) need not be “absorption” in the usual sense. Instead, it may be due to a lack of emitting material moving at that radial velocity. In fact, Ulrich has constructed models of inflowing “anti-winds” that have the property of producing such profiles! Despite these complications, essentially all giants later than spectral type K2 and supergiants later than about G5 do have obvious “circumstellar” absorption features that are blueshifted and broad compared with interstellar features and are generally interpreted as evidence for the presence of cool stellar winds. The violet displacement of this absorption in an intrinsically symmetrical emission line causes the violet (*V*) emission peak to be weaker than the redward (*R*) emission: in the literature this is called *V* < *R* asymmetry.

As summarized by Stencel and Mullan (1980*a, b*), the onset of massive cool winds, indicated by *V* < *R*

¹ Staff Member, Quantum Physics Division, National Bureau of Standards.

asymmetry, occurs at different locations in the H-R diagram depending on whether the Ca II or Mg II resonance lines are considered. This difference is particularly noticeable for giants and subgiants; Mg II $V < R$ asymmetries begin to occur in such stars about three spectral subclasses earlier than for the Ca II $V < R$ asymmetries. This phenomenon has still not been explained definitively. One additional source of confusion in the Mg II profiles is the presence of interstellar absorption components even in nearby stars (Böhm-Vitense 1981). Because of its lower cosmic abundance and greater depletion onto dust grains, Ca⁺ interstellar absorption is much weaker.

In many K giants and supergiants, e.g., α Boo (K2 III), the only direct evidence for a wind is the presence of $V < R$ asymmetry in the Mg II lines. In the late K giants, such as α Tau (K5 III), a similar asymmetry is also seen in the Ca II resonance lines. Cassinelli (1979), Castor (1981), and Hagen (1978), among others, have summarized the presence and methods for the analysis of other mass-loss indicators in luminous cool stars, such as infrared emission, radio emission, and direct imaging of the extended envelope in optical resonance lines, but none of these signatures of mass loss are present in the K giant stars. Thus, the only way of deriving quantitative information about mass loss such as mass-loss rates, velocity fields, temperature structures, and microturbulence in such stars is to model the Mg II lines. To our knowledge, there have been no systematic studies of cool winds by modeling these line profiles, although Chiu *et al.* (1977) applied a plane parallel, complete redistribution analysis to the study of the Mg II k line in α Boo, and Dupree (1982) has presented Ca II and Mg II profiles for an extended, expanding model of a star like β Dra (G2 Ib-II). Linsky (1980) has reviewed recent work on methods for inferring systematic velocity fields (outflow and inflow) from asymmetric line profiles.

Beginning with Deutsch's (1956) pioneering study of α Herculis, many authors have estimated mass-loss rates for individual luminous cool stars by analyzing one or several of the available mass-loss indicators. Unfortunately, these estimates differ by factors of 10^2 – 10^3 even for the well-observed M supergiants (cf. Hagen 1978; Goldberg 1979), and there are essentially no realistic estimates for the K giants. However, mass loss along the giant branch can have important consequences on the later stages of stellar evolution and the surface chemical composition of these stars. This topic has been reviewed by Renzini (1981) and Iben (1981), among others. Thus there is a critical need for accurate mass-loss rate measurements for late-type giants and supergiants.

In this paper we describe our method for solving the radiative transfer equation for chromospheric lines formed in late-type stellar winds. In § II we discuss our rationale for the selection of the comoving frame radiative transfer method for application to such expanding envelopes. In § III we consider the problem of redistribution of photons and discuss the sensitivity of the line profile to the assumed redistribution function

by reference to previous work on related subjects. In § IV we outline the basic logic of our adopted comoving frame (CMF), partial frequency redistribution (PRD) technique and its application to the case of a two-level atom. In § V, we give some examples to illustrate the sensitivity of the calculated line profiles to the most important physical and atomic parameters, and we summarize our conclusions in § VI.

II. MOVING ATMOSPHERE TECHNIQUES

There are essentially four ways of treating radiative transfer in atmospheres with velocity gradients: (i) Monte Carlo calculations, e.g., Magnan (1968), Slater, Salpeter, and Wasserman (1982); (ii) Sobolev or supersonic approximations, e.g., Sobolev (1957, 1960), Castor and Lamers (1979); (iii) observers' frame (OF) methods; and, (iv) comoving frame (CMF) methods. The choice of the best method for treating radiative transfer in the resonance lines formed in late-type giant winds is dictated by the following considerations:

(1) The winds are of low velocities with maximum values only 1–4 times the maximum *random* (microturbulent and thermal) velocity;

(2) the absorption wings and often portions of the emission feature are formed deep in the atmosphere, beneath the main systematic outflow region. Thus, to model these components of the line profiles, partial frequency redistribution (PRD) must be included (as is discussed in the next section);

(3) no direct information is available on the radial dependence of the outflow velocity, and theoretical models of extended cool star winds are still very schematic.

The first point excludes the Sobolev approximation, because the measured outflow velocities, V_{out} , of circumstellar components are typically $< \sim 50 \text{ km s}^{-1}$,² while microturbulent velocities, V_{Dopp} , as great as 20 km s^{-1} have been inferred in these objects. The Sobolev approximation cannot be used to model the spectral lines formed in such flows since one of its *necessary* conditions ($V_{\text{out}} > \sim \text{several } V_{\text{Dopp}}$) is not satisfied. Therefore, we must obtain "exact" solutions of the radiative transfer equation (RTE) with no *a priori* assumptions concerning the magnitude of the velocity fields. The second point means that an observer's frame (OF) (or inertial frame) formulation is impractical, since it would require the solution for a full angle- and frequency-dependent source function; solutions in the angle-averaged PRD approximation have been shown to yield incorrect results in an OF formulation (Magnan 1974; Mihalas *et al.* 1976). We have therefore adopted the comoving frame (CMF) (or fluid frame) formulation of the radiative transfer equation, wherein all the radiative transfer, assuming an angle-averaged redistribution function, is calculated in the moving rest frame, and the emergent profile is obtained from a final transformation into the observers'

² Three exceptions are the G supergiants α Aqr, β Aqr, and η Peg. The first two are hybrid stars (Hartmann, Dupree, and Raymond 1980), and all three have at least two distinct velocity components (three in β Aqr).

rest frame. Also, because of the great geometrical extent of the emitting regions involved, curvature effects must be included by solving the RTE in spherical geometry. We selected the comoving frame method as developed for spherical symmetry by Mihalas, Kunasz, and Hummer (1975) and Mihalas *et al.* (1976) as the most suitable for application to this specific problem. The original program was kindly supplied by Paul Kunasz and was modified to include PRD by the authors. It uses a Feautrier elimination scheme and can thus handle frequency-dependent line source functions (i.e., PRD). One limitation is that the velocity law must be monotonically increasing outward in order to satisfy an initial boundary condition on the violet edge of the profile. A short description of the CMF algorithm as applied in this study is given in § IV.

III. COMPLETE VERSUS PARTIAL REDISTRIBUTION

It has been recognized for some time that the assumption of complete frequency redistribution (CRD) of line photons by resonant scattering is incorrect for modeling the resonance lines formed in the chromospheres of late-type stars. Such lines have large radiative transition probabilities and, therefore, following photoexcitations, the excited ions will generally reradiate coherently (in their own rest frame) before the energy of the upper state is changed by elastic collisions. When the Doppler motions of these atoms are taken into account, and assuming that the scattering is isotropic, it is possible to derive a redistribution function (hereafter RF), $R_{II,A}(v', v)$, that is essentially the probability of an absorbed photon of frequency v' being re-emitted at a frequency v , where both frequencies are now in the stellar rest frame (Hummer 1962; Mihalas 1978). Since elastic collisions will occur before some ions reradiate, the actual RF can be assumed to be a linear combination of $R_{II,A}$ and of the CRD RF, where the fractional contribution of the latter is the ratio of the elastic to the total damping widths.

Using this formalism, several authors computed profiles of the resonance lines of Mg II and Ca II in the Sun (Milkey and Mihalas 1974; Shine, Milkey, and Mihalas 1975a; Heasley and Kneer 1976), in late-type dwarfs and giants (Milkey, Ayres, and Shine 1975; Shine, Milkey, and Mihalas 1975b; Ayres and Linsky 1975a; Kelch *et al.* 1978; Kelch, Linsky, and Worden 1979), and in supergiants (Basri 1980; Basri, Linsky, and Eriksson 1981), and they have discussed the effects on the line profiles of the two contrasting assumptions of partial redistribution (PRD) and CRD. All of these studies assumed static atmospheres. They produced in each case the usual self-reversed emission feature within absorption wings, but in the CRD profile the absorption wings are much brighter (in some cases, by almost an order of magnitude), and the Mg II k_1 and Ca II K_1 minima are therefore displaced farther from line center. For low-gravity stars with low chromospheric electron densities, these differential effects are enhanced, as expected, compared to those in the dwarfs like the Sun. In some cases, the K_2 emission peaks formed in CRD are also

noticeably stronger than their PRD counterparts, and as a consequence of the brighter emission peaks and wings, the full width at half-maximum of the K_2 features is typically greater in the CRD profile. The absorption cores for both PRD and CRD are generally identical, since Doppler redistribution dominates in both cases. The reason for the differing line profile shapes can be understood by a study of the dependence of the monochromatic line source functions on monochromatic optical depth (e.g., Milkey and Mihalas 1974). The wings are darker in PRD than in CRD because the PRD line source function at this frequency displacement, which is nearly pure coherent scattering, uncouples from the thermal source function deeper in the atmosphere and, as a consequence, is smaller than in the CRD case.

In modeling lines formed in early-type stars that have massive, high velocity ($V \gg V_{\text{Dopp}}$) winds, the CRD assumption is generally adopted, either implicitly (as in all studies utilizing the Sobolev approximation) or explicitly (e.g., Kunasz and Praderie 1981). This approximation is typically valid for these stars because the large macroscopic velocity fields produce systematic Doppler shifts of the different atmospheric layers with respect to each other. This influences the photon scattering redistribution far more than the intrinsic shape of the line profile. If "photospheric" absorption wings are present they are generally either subtracted from the observed profile before comparison is made with the theoretically computed profile, or accounted for as an actual boundary condition in some approximate way (see, e.g., Castor and Lamers 1979).

In cool stars lying above the main sequence, winds have much slower maximum velocities of 5–50 km s⁻¹ than those either in the solar case or in early-type stars. Since these stars have atmospheres intermediate between the two extreme cases of static and high velocity envelopes, it is important to study PRD effects on line profiles in the slow-moving outflow regime, where $V \lesssim \text{several} \times V_{\text{Dopp}}$ and V_{Dopp} includes both thermal and microturbulent motions.

Some theoretical studies have been published that compare the profiles produced in moving plane-parallel atmospheres using R_1 (pure coherent scattering in the atomic rest frame) and CRD. Cannon and Vardavas (1974) found, for an outflow velocity equal to the thermal velocity, that there are important qualitative differences between the profiles. However, Magnan (1974) and Mihalas *et al.* (1976) showed that these large effects are spurious, due to the incorrect use of angle-averaged RFs in an observer's frame calculation,³ and that there is essentially no difference between the profiles computed for the two different RFs when they used a comoving frame method (in which it is appropriate to assume angle-averaged RFs). The only previous comparison that

³ The radiation emitted isotropically in a region moving with some systematic velocity relative to an external observer is seen by this observer to be anisotropic (angle-dependent), and the asymmetry increases as the velocity becomes greater. Thus, to do this problem correctly in the observer's frame method requires using full angular and frequency dependent redistribution functions.

we are aware of between the line profiles in spherical, moving atmospheres resulting from the contrasting assumptions of angle-averaged R_{II} PRD and of CRD was made by Peraiah (1979), but these calculations were also done in the observer's frame and thus may not be appropriate.

On the basis of previous work, we expect the difference between PRD and CRD profiles of resonance lines will be enhanced: (a) as the ratio of systematic to turbulent velocities decreases, and (b) when the emission is due primarily to an effectively thick chromosphere, rather than to the formation region of the line having a greater effective area than that of the neighboring continuum, i.e., "P Cygni"-type emission. In a given line profile, the absorption wings will generally be formed deep enough in the atmosphere that they are not influenced by the systematic velocity field in the chromosphere, and hence the results of the static PRD versus CRD studies should be applicable. Since, in a strong line such as Mg II k , these wings form a dark background against which the emission is measured, comparison of observed with computed CRD profiles can yield an incorrect estimate of the true emission measure. Such comparisons will also generally lead to underestimates of the temperature in the temperature minimum region of the atmosphere, since CRD analyses usually overestimate the flux level in the absorption wings.

IV. SOLUTION OF THE RADIATIVE TRANSFER EQUATION

A good review of the solution of the radiative transfer equation (hereafter RTE) in the comoving or fluid frame is given by Mihalas (1978). The general procedure is to include only the Doppler shift effects on the line photon frequencies and to ignore the second-order effects of advection and aberration, which Mihalas, Kunasz, and Hummer (1976a) found to be negligible in stellar wind situations. The RTE and related moment equations are solved in the fluid frame where an observed frequency ν corresponds to a local comoving frequency $\nu_0 = \nu(1 - \mu V/c)$, where V is the outflow velocity, c the speed of light, and μ the usual direction cosine factor between the velocity vector and the observer. To account for the velocity field, an additional term $\propto \partial I^0 / \partial \nu^0$ appears in the RTE. To solve this partial differential equation, the differentials are replaced by differences, and the resultant system of algebraic equations is solved using a standard Feautrier algorithm. The usual boundary and initial conditions are (1) no incoming radiation at the upper boundary, (2) thermalization of source functions at the lower boundary, and (3) zero gradient in the intensity ($\partial I / \partial \nu = 0$) at the highest frequency point in the line.

The actual solution of the RTE is iterative, as discussed by Mihalas and Kunasz (1978). A ray-by-ray formal solution of the RTE in the CMF is performed, and then the Eddington factors at each frequency ν and depth point d are calculated from the derived radiation field. Knowing these factors, we solve the moment equations and obtain improved values of the mean intensity and source function at each point in the (ν, d) grid. Using the latter, we obtain a new formal RTE solution, and

obtain improved Eddington factors. This process converges rapidly, and usually achieves 1% agreement within three or four iterations. Given the source functions and opacities calculated in the CMF and the velocity field, we then compute the emergent line profile in the observer's frame. As discussed by Mihalas, Kunasz, and Hummer (1976b) and Mihalas and Kunasz (1978), care must be taken in setting up an appropriate grid of impact parameters and OF frequencies, and an additional inaccuracy of $\lesssim 1\%$ may be expected due to the need to interpolate desired quantities from the CMF grid of points.

We have modified the CMF code developed by P. Kunasz to take into account PRD effects. This involved replacing frequency independent CRD line source functions by monochromatic PRD ones and replacing the CRD weights in the scattering integral by those appropriate for PRD. The form of the redistribution function is (cf. Basri 1980)

$$R(\nu', \nu) = \tilde{\Lambda} \phi_{\nu'} \phi_{\nu} + (1 - \tilde{\Lambda}) R_{II}(\nu', \nu), \quad (1)$$

where the formula for R_{II} is given in Hummer (1962) and the corresponding weights needed in the scattering integral are generated as in Basri (1979, 1980) from interpolation of a table of values constructed from *exact* integrations of the redistribution function, ϕ_{ν} is a normalized Voigt profile, and $\tilde{\Lambda}$ is the modified incoherence fraction defined by

$$\tilde{\Lambda} = \frac{\Lambda + a_c}{1 + a_c}, \quad (2)$$

where

$$\Lambda = \frac{\Gamma_e}{\Gamma_R + \Gamma_e + \Gamma_I}. \quad (3)$$

The Γ s are damping widths of the upper state for radiative (R) transitions, elastic (e), and inelastic (I) collisional transitions, while a_c is a correction factor for situations such as in Ca II, where there is an alternate radiative decay path other than to the ground state that introduces a minimum value for the incoherence.

In equation (1) we have substituted for the exact Doppler redistribution function, R_{III} , the simpler CRD approximation, since this has been shown to be an adequate representation for R_{III} (Frisch 1980; Vardavas 1976). We have *not* represented R_{II} by the Kneer (1975) approximation, because Basri (1980) has shown it to be a poor representation of the exact function in the low density atmospheres of cool, luminous stars, which produces profiles significantly different from those calculated using the exact R_{II} expression.

The redistribution will be depth-dependent because of two effects:

(1) The line profile adopted is a Voigt profile, which is a function of the Doppler broadening and total damping widths. Both of these quantities can depend on radial distance, which makes the line profile at a given frequency displacement also depth dependent.

(2) The incoherence fraction is also a function of the

damping widths and hence is depth dependent. At high densities (in and below the photosphere) $\bar{\Lambda} \rightarrow 1$, while at low densities $\bar{\Lambda} \rightarrow a_c$ (≈ 0.07 for Ca II *K*, for example, and 0 for Mg II *k*).

We used a simple two-level atom where the two levels represent the upper and lower states of the resonance line in question. Following Heasley and Kneer (1976) and Mihalas (1978, see his eq. [13–92]), we have for the monochromatic line source function

$$S_L^\nu = (1 - \epsilon) \left[\phi_\nu^{-1} \int R(\nu', \nu) J_{\nu'} d\nu' \right] + \epsilon B_\nu, \quad (4)$$

where $\epsilon = N_e C_{21}/(A_{21} + N_e C_{21})$. It is implicitly assumed that the stimulated emission profile is identical to the absorption profile in this equation. This form of S_L^ν permits us to solve the transfer equation in one step without the need for iterations. In the actual calculations we have represented the integral in equation (4) by a summation, i.e.,

$$\phi_\nu^{-1} \int R(\nu', \nu) J_{\nu'} d\nu' \approx \sum_j W(\nu_j, \nu) J_{\nu_j}, \quad (5)$$

where the weights W are obtained as discussed above. The complete source function at a frequency ν is then

$$S_\nu = \frac{\kappa_L^{\text{IND}} S_L^\nu \phi_\nu + \eta_c^\nu}{\kappa_L^{\text{IND}} \phi_\nu + \kappa_c^\nu}, \quad (6)$$

where κ_L^{IND} is the frequency-independent opacity, ϕ_ν is the previously discussed absorption profile, which is fixed for a given radius and frequency, and η_c^ν and κ_c^ν are the net continuum emissivity and opacity, respectively, including electron scattering terms. The line absorption coefficient κ_L^{IND} is calculated from the standard formula (e.g., Kunasz and Praderie 1981, eq. [4]) and since we do not include a stimulated emission correction, it is directly proportional to the population of the lower level (the ground state). The latter is obtained from a simple ionization calculation, assuming that the ground state population is equal to the total population of the ion, and remains fixed during the main iteration cycle.

One additional complication introduced by PRD is in the conversion back into the observer's frame. In CRD, S_L is essentially independent of frequency across the line profile and is thus only a function of radial distance, while in PRD the source function depends on both frequency and radial distance. Thus, the Doppler shift $\nu' - \nu = \nu(\mu V/c)$ between the comoving frame and the stationary observer's frame must be taken into account carefully, since $S_L(\nu) \neq S_L(\nu')$.

V. SAMPLE RESULTS ILLUSTRATING PROFILE SENSITIVITY TO INPUT PARAMETERS

In subsequent papers, we shall discuss the application of these techniques to the analysis of actual stellar profiles. For the present, we give some examples of computed line profiles generated for rather schematic atmospheres, in order to show the influence of varying the following input parameters: the maximum outflow

velocity (V_{max}), the outer radius of the expanding envelope (R_{max}), the temperature gradient of the chromospheric rise from the temperature minimum $[(dT/d\tau)]$, the ratio of line to continuum opacities (κ_L/κ_c), and the degree of frequency redistribution ($\bar{\Lambda}$).

In order to verify that our results give the correct behavior in PRD and CRD for the limiting cases of expansion velocity $V_{\text{exp}} \rightarrow 0$ (static atmosphere) and $V_{\text{exp}} \rightarrow \text{many} \times V_{\text{Dopp}}$ (Sobolev limit), we first chose a particularly simple temperature structure: for continuum optical depth, $\tau_c > \frac{2}{3}$, we fix $T(\tau_c) = T_{\text{eff}}$, while for $\tau_c \leq \frac{2}{3}$, we have $T(\tau_c)$ monotonically increasing with decreasing τ_c . Such an atmosphere will not produce any "photospheric" absorption wings, hence any emission or absorption must originate in the chromosphere. In this and all subsequent examples, we included no macro-turbulent, rotational, or instrumental broadening effects.

In Figure 1, we present the line profiles produced in such an atmosphere of maximum extent $R_{\text{max}} = 10R_*$, where R_* is the photospheric radius, for the two extreme cases $V_{\text{max}} = 0$ and $V_{\text{max}} = 6 \times V_{\text{Dopp}}(R_{\text{max}})$, and for the two contrasting assumptions of PRD ($\bar{\Lambda} \approx 0$) and CRD ($\bar{\Lambda} = 1$). The static case, while physically unrealistic, is the simplest one to compare with previous calculations (e.g., Fig. 1 of Milkey, Ayres, and Shine 1975; and Fig. 1 of Shine, Milkey, and Mihalas 1975b). The effects on the line wings are essentially identical to those found by these authors. The CRD wings are brighter than in PRD because collisional redistribution much more strongly couples the wing source function to that of the core. The PRD emission feature is also noticeably narrower than the CRD feature. The shape of the central absorption is different in the present calculations compared with the previous ones due to the large spherical extent of the atmosphere, which produces very deep self-absorption. Since in the core the redistribution is primarily Doppler, there is negligible difference between the CRD and PRD cores as is expected since we have approximated R_{III} by the CRD function. Because of this broad, deep absorption, the PRD emission peaks are never as high as the CRD peaks, contrary to the plane-parallel profiles computed in the two quoted references. There is, as a result, a fairly considerable difference in equivalent widths for the two contrasting cases, 0.40 Å for PRD compared to -0.60 Å in the CRD case, where the minus sign indicates net emission.

As the velocity of the outflow increases, we expect that the redistribution assumption should become less and less critical, since the major photon escape mechanism will be the systematic Doppler shifts of the various regions of the chromosphere relative to one another (i.e., a Sobolev-type mechanism) rather than to their redistribution within the line profile. In the Sobolev limit, in fact, the emergent line profile shape should be independent of the assumed intrinsic profile shape or redistribution mechanism. Castor and Lamers (1979) have computed P Cygni-type line profiles for a range of atmospheric properties in the Sobolev approximation. In Figure 1 we also show the PRD and CRD profiles

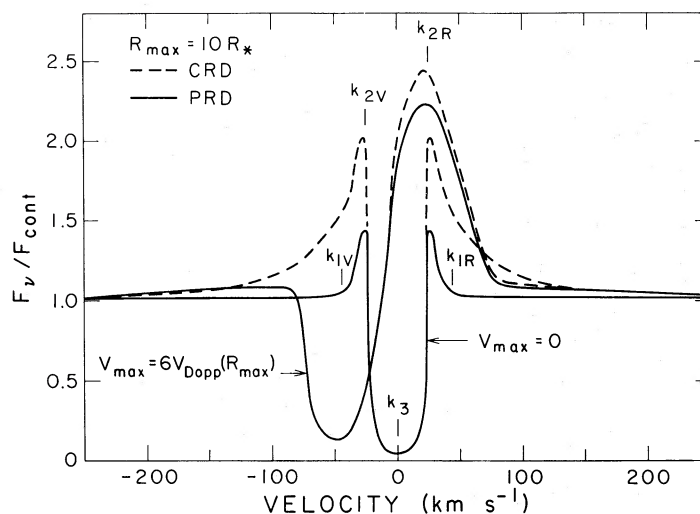


FIG. 1.—Computed profiles for an atmosphere with maximum extent $10 R_*$ for the two limiting cases of no expansion ($V_{\max} = 0$) and high velocity expansion [$V_{\max} = 6V_{\text{Dopp}}(R_{\max})$]. Differences between the PRD and CRD profiles are indicated. The location of the minimum and maximum features described in the text for the Mg II k line are indicated by their usual symbols.

for an atmosphere where $V_{\max} = 6 \times V_{\text{Dopp}}(R_{\max})$ in the outer envelope. The different RF assumptions now produce exactly the same emergent profile, showing that the Sobolev limit has been nearly attained, except at the emission peak where the CRD profile is 10% brighter. (The sense of this difference is still the same as for the static and slow-moving cases.) Thus the qualitative behavior of the contrasting line profiles predicted by R_{II} PRD and by CRD agrees with previous work in the asymptotic limits of $V \rightarrow 0$ and $V \rightarrow \text{many} \times V_{\text{Dopp}}$.

In realistic late-type stars, most chromospheric resonance lines are superposed on much broader photospheric absorption lines. In order to duplicate this more complex situation, we henceforth adopt a more realistic temperature structure. For $\tau_c > \tau_1$, we assume an Eddington-type functional dependence of temperature, i.e.,

$$T(\tau_c) = T_{\text{eff}}^4 \left(\frac{3}{4} \tau_c + \frac{1}{2} \right), \quad (7)$$

while for $\tau_2 < \tau_c < \tau_1$, we adopt

$$T(\tau_c) = T_{\text{eff}}(a_1 \log \tau_c + a_2), \quad (8)$$

and for $\tau_c < \tau_2$ we fix $T(\tau_c) = 1.5 \times T_{\text{eff}}$. The constants a_1 and a_2 were fixed by enforcing continuity of the $T - \tau_c$ relation at the transition depths τ_1 and τ_2 . In order to emphasize the chromospheric emission relative to the P Cygni emission, we have chosen a rather large value of $\tau_1 = 0.1$.

We have also adopted a microturbulent velocity that increases logarithmically with radius from 2 km s^{-1} in the photosphere ($r = R_*$) to a maximum of 10 km s^{-1} at $2 R_*$. We have assumed that the systematic outflow commences in the vicinity of the temperature minimum region, i.e., just above the photosphere, and that at greater radial distance it is always proportional to the local Doppler velocity. Thus, a model described as

$V = 3 \times V_{\text{Dopp}}$ will have a velocity law that also increases linearly with $\log r$ for $r \gtrsim R_*$ and reaches 30 km s^{-1} at $2 R_*$. For $r \lesssim R_*$, hydrostatic equilibrium is presumably valid and the pressure and density should decrease exponentially with increasing radial distance. Since we are using the equation of continuity as the constraint on density in this region, the velocity must decrease exponentially inward so as to produce the correct density dependence. We ensure a smooth fit between the two velocity law regimes. We have chosen stellar parameters $T_{\text{eff}} = 4250 \text{ K}$, $R_* = 26 R_{\odot}$, and a photospheric density distribution similar to such an early K giant as Arcturus (K2 III), and have used atomic parameters such as transition probabilities, collision strengths, and collisional damping widths appropriate for the Mg II k line. We have adopted an effective collision strength for this line of 10.6 (Mendoza 1981), a Stark width $\Gamma_s = 1.6 \times 10^{-6} N_e T_5^{-0.3}$ (Barnes 1971), and a van der Waals width $\Gamma_v = 1.3 \times 10^{-8} N_{\text{HI}} T_5^{0.3}$ (Shine 1973; Ayres and Linsky 1976), where $T_5 = (T_e/5 \times 10^3 \text{ K})$ and N_e and N_{HI} are the population densities of electrons and neutral hydrogen, which are calculated from the total density using a simple ionization equilibrium algorithm.

In Figure 2, we demonstrate the effects of changing the assumed outflow velocity law on the emergent line profile produced by this more realistic outer atmosphere. The relative behavior of the CRD and PRD profiles in Figure 2 is similar to what was previously seen in Figure 1, although because the chromosphere emission width is much greater than the P Cygni width, even in the $V_{\max} = 3V_{\text{Dopp}}(R_{\max})$ example, there is considerable difference between the profiles for the two redistribution assumptions. Since in late-type luminous stars the full widths of the Mg II k lines are very large ($150\text{--}500 \text{ km s}^{-1}$) compared to the outflow velocities (typically $5\text{--}50 \text{ km s}^{-1}$), large errors in the derived atmospheric

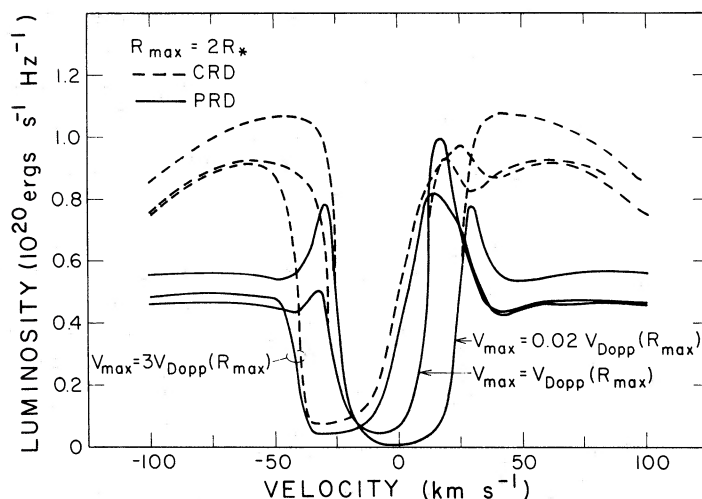


FIG. 2.—Computed profiles of the Mg II k line for an early K giant star with $R_{\max} = 2 R_{\star}$. CRD and PRD profiles are given for three different velocity laws.

properties would certainly result from comparing CRD profiles to observed profiles. In particular, the emission features are much more luminous when one assumes the incorrect CRD redistribution function.

In Figure 3 we examine how the profiles change by varying the outer radius of the expanding region for the case of an envelope with $V = V_{\text{Dopp}}$ everywhere above the temperature minimum. The conclusion that can be drawn about these profiles is that both the emission and absorption components become more pronounced with increasing R_{\max} . Again, one computes far too much emission by assuming CRD.

In Figure 4, we compare the resultant profiles as the value of $(dT/d\tau)$ in the chromosphere increases for the

same velocity structure. This is done by moving the optical depth τ_2 where the atmosphere reaches its maximum temperature inward from $\tau_c = 10^{-3}$ to $10^{-2.5}$, and finally to 10^{-2} . The chromospheric emission strengthens as $dT/d\tau$ increases, but unlike the previous examples, the absorption feature also becomes shallower. The CRD assumption is also more inaccurate for large $dT/d\tau$, since the difference between the coherent scattering source function and the CRD source function in the temperature rise region is more pronounced in this case. The emission due to the chromospheric temperature rise is very broad, since we have started the rise at a very large optical depth, and it is clearly separable, in the steepest $dT/d\tau$ case assuming CRD,

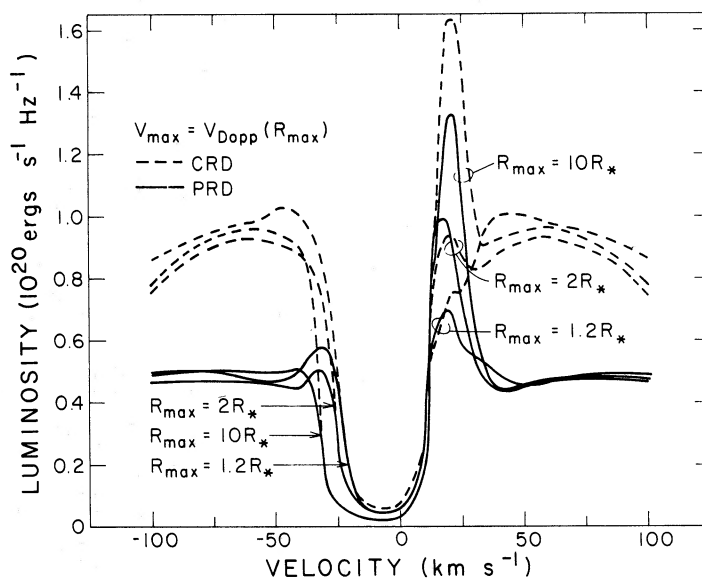


FIG. 3.—Computed profiles of the Mg II k line for an early K giant star with $V_{\max} = V_{\text{Dopp}}(R_{\max})$ for radial extents of the chromosphere of $1.2 R_{\star}$, $2 R_{\star}$, and $10 R_{\star}$.

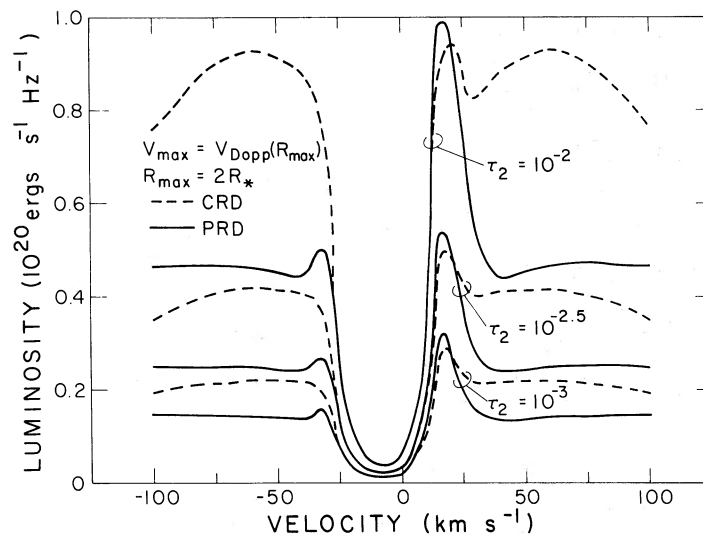


FIG. 4.—Computed profiles of the Mg II k line for an early K giant star keeping $V_{\max} = V_{\text{Dopp}}(R_{\max})$ and $R_{\max} = 2 R_*$, but changing the chromospheric temperature gradient ($dT/d\tau$) by varying the optical depth τ_2 where the atmosphere reaches its maximum temperature.

from the emission due to the geometric extension of the envelope. The FWHM of the P Cygni emission feature is essentially of the order of the sum of the maximum systematic and random velocities ΣV , and, given the adopted parameters in this example, is much narrower than the chromospheric emission feature. The PRD and CRD profiles are nearly identical in the absorption core, which is blueshifted by $\sim \Sigma V$, as the core is now a composite of P Cygni absorption and chromospheric self-absorption. This is as expected since Doppler effects dominate the line core for each type of redistribution.

The wings of the PRD profile are much darker than the CRD wings in every case considered; this is due to

the line source function at large wavelength displacements becoming decoupled from the local Planckian value at a much deeper point in the atmosphere in PRD than in CRD. Thus, the PRD wing source function has no significant maximum in the vicinity of the steep temperature rise (as in CRD), but remains nearly flat, producing relatively dark, flat wings in the emergent line profile.

Finally, we illustrate in Figure 5 the effect on the emergent flux profile of decreasing the ratio of the line-to-continuum opacity κ_L/κ_C by a factor of 3, which is equivalent to an abundance decrease of the same factor. As might be anticipated, the central absorption is

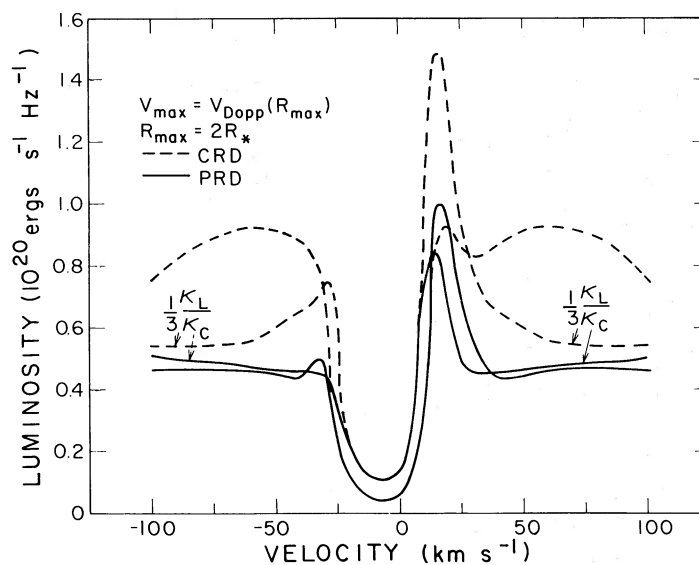


FIG. 5.—Computed profiles of the Mg II k line for an early K giant star keeping $V_{\max} = V_{\text{Dopp}}(R_{\max})$ and $R_{\max} = 2 R_*$, but for the nominal and $\frac{1}{3}$ nominal value of the line-to-continuum opacity ratio.

narrower and less deep and the PRD redward peak is weaker. The increased luminosity of the CRD red peak is a consequence of the decrease in the line opacity corresponding to a given continuum optical depth (and hence temperature), which moves the chromospheric emission closer to line center where it combines with the P Cygni emission peak to produce a narrower peak with a higher maximum flux.

VI. CONCLUSIONS

In this paper we have described our methods for computing emission-line profiles in extended, expanding chromospheres of late-type stars, and have illustrated the sensitivity of the computed profiles to the assumed atmospheric and wind parameters. The purpose of these calculations is to develop some physical insight concerning the information contained in these asymmetric line profiles prior to deriving in subsequent papers the parameters for chromospheric winds in specific stars by matching computed and observed profiles of such resonance lines as Mg II *h* (2803 Å) and *k* (2796 Å), Mg I 2852 Å, and O I 1302, 1305, 1306 Å. Our conclusions are as follows:

(1) One must properly include the physics of coherent scattering in the rest frame of the atom and solve the radiative transfer equation in an approximation that accurately describes this scattering. Since late-type giants and supergiants have extended geometries and winds that are expanding at only a few times the Doppler velocity, we find that we must solve the transfer equation for spherical geometry in the comoving (or fluid) frame, and use the partial redistribution (PRD) redistribution function that includes coherent scattering in the atom's rest frame, Doppler redistribution, and a small component of complete redistribution (CRD) due to elastic scattering. Observer's frame calculations and the Sobolev approximation are inappropriate for this class of problems.

(2) We find that the PRD profiles differ greatly from the physically unrealistic CRD profiles in all cases considered except when we assume that the maximum expansion velocity, V_{\max} , is ≥ 6 times the Doppler velocity, $V_{\text{Dopp}}(R_{\max})$. In this case one is close to the regime where the Sobolev approximation is valid and the PRD and CRD profiles are nearly identical. Also the absorption cores are identical in PRD and CRD for all

cases because the redistribution is Doppler in both approximations. The sense of the difference between the PRD and CRD profiles is that the emission features in CRD are too broad and luminous and the CRD wings are too bright. We conclude that one would derive very erroneous parameters for the stellar chromosphere and wind by attempting to match observed profiles with computed CRD profiles.

(3) For models of all degrees of extension, we find that the effect of increasing V_{\max} is to produce a blue-shifted absorption feature and a more luminous red emission peak.

(4) The effect of increasing the amount of atmospheric extension, as measured by R_{\max}/R_* , is to make the red emission peak more luminous and the absorption core darker and broader. Our PRD profiles for large V_{\max} and R_{\max}/R_* show red emission peaks that are very broad and luminous.

(5) We find that increasing the chromospheric temperature gradient brightens both the red and violet emission peaks, and that decreasing the line-to-continuum opacity ratio causes the red emission peak to become less bright and the absorption feature to become less deep and narrower.

In subsequent papers, we will apply the analytical techniques discussed here to modeling the ultraviolet resonance line profiles in a variety of late-type giants and supergiants. Our aim is to obtain meaningful estimates of the mass loss rates, velocity laws, and chromospheric sizes for a sample of cool giants and supergiants in order to test the predictions of the different mass loss acceleration mechanisms (cf. Castor 1981; Linsky 1981; Hartmann and MacGregor 1980) that are now being seriously considered.

We wish to thank Dr. P. Kunasz for a great deal of help in revising existing computer codes to include PRD. We gratefully acknowledge the support of the National Aeronautics and Space Administration through grants NGL 06-003-057 and NAG 5-82 to the University of Colorado. The computations for this paper were done on the Cray-1 computer at the National Center for Atmospheric Research, under contract with the National Science Foundation. We wish to thank the staff of the NCAR computing center for assistance in this project.

REFERENCES

- Avrett, E. H., and Hummer, D. G. 1965, *M.N.R.A.S.*, **130**, 295.
 Ayres, T. R., and Linsky, J. L. 1975a, *Ap. J.*, **200**, 660.
 ———. 1975b, *Ap. J.*, **201**, 212.
 ———. 1976, *Ap. J.*, **205**, 874.
 Barnes, K. S. 1971, *J. Phys. B*, **4**, 1377.
 Basri, G. S. 1979, Ph.D. thesis, University of Colorado.
 ———. 1980, *Ap. J.*, **242**, 1133.
 Basri, G. S., Linsky, J. L., and Eriksson, K. 1981, *Ap. J.*, **251**, 162.
 Beals, C. S. 1951, *Pub. Dom. Ap. Obs.*, **9**, 1.
 Böhm-Vitense, E. 1981, *Ap. J.*, **244**, 504.
 Cannon, C. J., and Vardavas, I. M. 1974, *Astr. Ap.*, **32**, 85.
 Cassinelli, J. P. 1979, *Ann. Rev. Astr. Ap.*, **17**, 275.
 Castor, J. I. 1981, in *Physical Processes in Red Giants*, ed. I. Iben, Jr. and A. Renzini (Dordrecht: Reidel), p. 285.
 Castor, J. I., and Lamers, H. J. G. L. M. 1979, *Ap. J. Suppl.*, **39**, 481.
 Chiu, H. Y., Adams, P. J., Linsky, J. L., Basri, G. S., Maran, S. P., and Hobbs, R. W. 1977, *Ap. J.*, **211**, 453.
 Deutsch, A. J. 1956, *Ap. J.*, **123**, 210.
 Dupree, A. K. 1982, in *Advances in Ultraviolet Astronomy: Four Years of IUE Research*, ed. Y. Kondo, J. M. Mead, and R. D. Chapman (NASA Conf. Publ. 2238), p. 3.
 Frisch, H. 1980, *Astr. Ap.*, **83**, 166.
 Goldberg, L. 1979, *Q.J.R.A.S.*, **20**, 361.
 Hagen, W. 1978, *Ap. J. Suppl.*, **38**, 1.
 Hartmann, L., Dupree, A. K., and Raymond, J. C. 1980, *Ap. J. (Letters)*, **236**, L143.
 Hartmann, L., and MacGregor, K. B. 1980, *Ap. J.*, **242**, 260.
 Heasley, J. N., and Kneer, F. 1976, *Ap. J.*, **203**, 660.

- Hummer, D. G. 1962, *M.N.R.A.S.*, **125**, 21.
- Iben, I. Jr. 1981, in *Effects of Mass Loss on Stellar Evolution*, ed. C. Chiosi and R. Stalio (Dordrecht: Reidel), p. 373.
- Kelch, W. L., Linsky, J. L., Basri, G. S. Chiu, H. Y., Chang, S. H., Maran, S. P., and Furenlid, I. 1978, *Ap. J.*, **220**, 962.
- Kelch, W. L., Linsky, J. L., and Worden, S. P. 1979, *Ap. J.*, **229**, 700.
- Kneer, F. 1975, *Ap. J.*, **200**, 975.
- Kunasz, P. B., and Praderie, F. 1981, *Ap. J.*, **247**, 949.
- Linsky, J. L. 1980, *Ann. Rev. Astr. Ap.*, **18**, 439.
- . 1981, in *Effects of Mass Loss on Stellar Evolution*, ed. C. Chiosi and R. Stalio (Dordrecht: Reidel), p. 187.
- Magnan, C. 1968, *Ap. Letters*, **2**, 213.
- . 1974, *Astr. Ap.*, **35**, 233.
- Mendoza, C. 1981, *J. Phys. B*, **14**, 2465.
- Mihalas, D. 1978, *Stellar Atmospheres* (San Francisco: Freeman), p. 422.
- Mihalas, D., and Kunasz, P. B. 1978, *Ap. J.*, **219**, 635.
- Mihalas, D., Kunasz, P. B., and Hummer, D. G. 1975, *Ap. J.*, **202**, 465.
- . 1976a, *Ap. J.*, **206**, 515.
- . 1976b, *Ap. J.*, **210**, 419.
- Mihalas, D., Shine, R. A., Kunasz, P. B., and Hummer, D. G. 1976, *Ap. J.*, **205**, 492.
- Milkey, R. W., Ayres, T. R., and Shine, R. A. 1975, *Ap. J.*, **197**, 143.
- Milkey, R. W., and Mihalas, D. 1974, *Ap. J.*, **192**, 769.
- Peraiah, A. 1979, *Kodaikanal Obs. Bull., Series A*, **2**, 203.
- Renzini, A. 1981, in *Effects of Mass Loss on Stellar Evolution*, ed. C. Chiosi and R. Stalio (Dordrecht: Reidel), p. 319.
- Rydgren, A. E. 1977, *Pub. A.S.P.*, **89**, 557.
- Shine, R. A. 1973, Ph.D. thesis, University of Colorado.
- Shine, R. A., Milkey, R. W., and Mihalas, D. 1975a, *Ap. J.*, **199**, 724.
- . 1975b, *Ap. J.*, **201**, 222.
- Slater, G., Salpeter, E. E., and Wasserman, I. 1982, *Ap. J.*, **255**, 293.
- Sobolev, V. V. 1957, *Soviet Astr.*, **1**, 678.
- . 1960, *Moving Atmospheres of Stars*, trans. by S. Gaposchkin (Cambridge, MA: Harvard University Press).
- Stencel, R. E., and Mullan, D. J. 1980a, *Ap. J.*, **238**, 221.
- . 1980b, *Ap. J.*, **240**, 718 (addendum).
- Ulrich, R. K. 1976, *Ap. J.*, **210**, 377.
- Vardavas, I. M. 1976, *J. Quant. Spectrosc. Rad. Transf.*, **16**, 715.

STEPHEN A. DRAKE: Joint Institute for Laboratory Astrophysics, University of Colorado, Boulder, CO 80309

JEFFREY L. LINSKY: Joint Institute for Laboratory Astrophysics, University of Colorado, Boulder, CO 80309